

# Design of a Broadband Polarization Controller Based on Silicon Nitride-Loaded Thin-Film Lithium Niobate

Jiří Čtyrský<sup>1,2\*</sup>, Ivan Richter<sup>2</sup> and Jiří Petráček<sup>3,4</sup>

<sup>1</sup> CAS Institute of Photonics and Electronics, Chaberská 57, 18251 Prague, Czech Republic

<sup>2</sup> Faculty of Nuclear Sciences and Physical Engineering, Czech Technical University in Prague, Břehová 7, 11519 Prague 1, Czech Republic

<sup>3</sup> Faculty of Mechanical Engineering, Brno University of Technology, Technická 2896/2, 61669 Brno, Czech Republic

<sup>4</sup> Central European Institute of Technology, Brno University of Technology, Purkyňova 656/123, 61200 Brno, Czech Republic

\* ctyrsky@ufe.cz

**Polarization controller is designed on Si<sub>3</sub>N<sub>4</sub>-loaded thin film LiNbO<sub>3</sub>. Broadband operation in the wavelength band from 1.45 to 1.65 μm is achieved by using a mode evolution TM/TE splitter/converter, two mode evolution 3-dB couplers and two electro-optic phase shifters. A single TE-mode output can be achieved by applying control voltages lower than 5 V for any input polarization state.**

**Keywords:** Polarization control, mode evolution splitter, broadband 3-dB couplers

## INTRODUCTION

Polarization controllers are important components of optical communication systems. Integrated-optic polarization controllers in Ti:LiNbO<sub>3</sub> waveguides have been described already several decades ago [1]. Recent development of the lithium niobate on insulator (LNOI) technology [2] allows to design more compact electro-optic devices with lower control voltage [3]. Our design, although similar to that described in [3], was proposed independently and differs in several features. Firstly, we choose the silicon nitride-loaded LNOI waveguides [4, 5] as an alternative to LiNbO<sub>3</sub> rib waveguides in order to avoid uneasy etching of the LiNbO<sub>3</sub> crystal. Secondly, to ensure broadband operation, we implemented an adiabatic mode evolution TM/TE coupler [6] as a polarization splitter/converter, and thirdly, mode evolution 3-dB couplers, somewhat similar to those described in [7] and [8], are designed. An X-cut LiNbO<sub>3</sub> slab is chosen for efficient electro-optic phase shifting. Numerical simulations by COMSOL Multiphysics and the proprietary Fourier modal method [9] predicted the total loss in the polarization controller of about 0.5 dB in the range from 1.45 to 1.65 μm. The operation voltage of phase shifters, required to direct the full input power to the single TE<sub>00</sub> mode of the output port, was found to be lower than 5 V.

## PROPERTIES OF Si<sub>3</sub>N<sub>4</sub>-LOADED LNOI WAVEGUIDES

The thickness of the LiNbO<sub>3</sub> slab was chosen as 400 nm, the Si<sub>3</sub>N<sub>4</sub> layer is 300 nm thick. Air is used as an upper cladding, since any higher-index overlayer reduces the strength of the required TM/TE coupling. The dispersion and radiation loss curves of the waveguides oriented along the Y-axis of the LiNbO<sub>3</sub> crystal are shown in Figs. 1(a) and 1(b), respectively. The waveguide cross-section is shown in the inset of Fig. 1(b). Fig. 1(c) shows the angular dependences of the effective refractive indices for propagation declined from the crystal Y-axis by an angle. Results were calculated for the wavelength of 1550 nm using COMSOL mode solver.

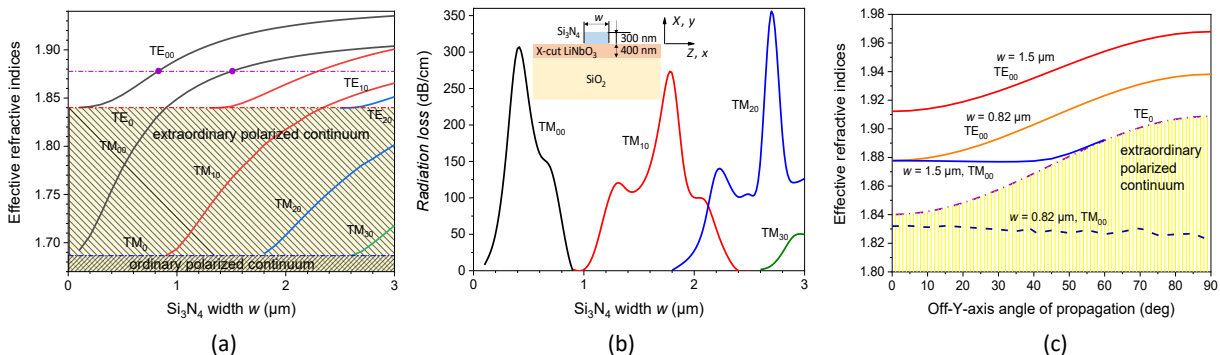


Fig. 1. Dispersion properties of the Si<sub>3</sub>N<sub>4</sub>-loaded LNOI waveguides. X, Z are crystal axes of the LiNbO<sub>3</sub> slab, x, y are coordinates.

The TE modes propagate without radiation into the LiNbO<sub>3</sub> slab since their effective indices are larger than the effective index of the planar TE<sub>0</sub> mode of the LiNbO<sub>3</sub> crystal slab. The TM modes—although predominantly ordinary polarized—are free of radiation losses only for wide enough waveguides.

## POLARIZATION CONTROLLER

The configuration of the polarization controller is schematically shown in Fig. 2. The TE-polarized input mode propagates through the TM/TE splitter/converter essentially unaffected, while the TM-polarized mode is converted into the TE mode of the bottom waveguide. Two cascaded combinations of the phase shifter and the 3-dB coupler are used to coherently combine the TE-polarized fields from both output ports of the TM/TE splitter/converter into a single output port. It can be easily shown that by proper adjustment of the relative phase of inputs of any (lossless) 3-dB coupler, the amplitudes in both output ports can be equalized. The second phase shifter is used to adjust the relative phase so that both input waves are coherently superposed in one of the output ports of the second 3-dB coupler. The control voltages  $U_{eq}$  and  $U_c$  of the phase shifters can thus be optimally adjusted by minimizing the output from the other port.

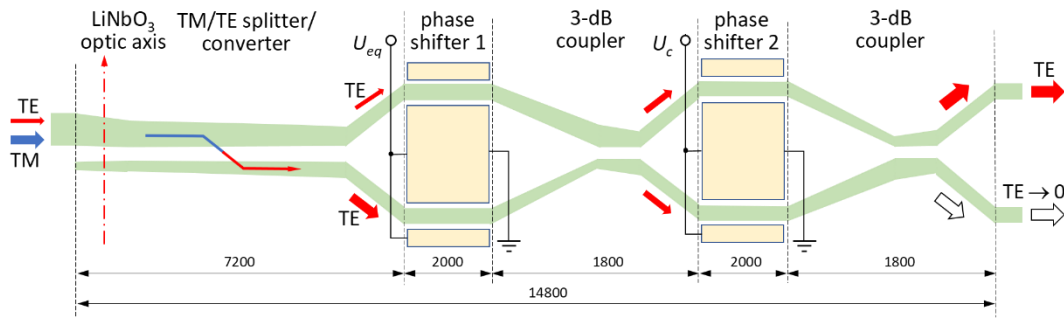


Fig. 2. Configuration of the polarization controller.

## ADIABATIC MODE EVOLUTION TM/TE COUPLER

The design of an adiabatic mode evolution TM/TE coupler started with the observation that the effective indices of the  $TE_{00}$  mode of the waveguide of the width of  $0.8 \mu\text{m}$  and of the  $TM_{00}$  of the waveguide of the width of  $1.5 \mu\text{m}$  are nearly identical (see the violet dots in Fig. 1(a)). If these waveguides come close to each other, the modes get hybridized due to the 3D vector character of their electric fields. This is reflected by the appearance of the avoided crossing of their dispersion curves [6] which corresponds to the polarization conversion during the mode evolution. The spectral position of the avoided crossing depends on the waveguide widths and on their separation. Proper adiabatic shaping of the coupler is required to ensure efficient polarization conversion in the required wavelength band.

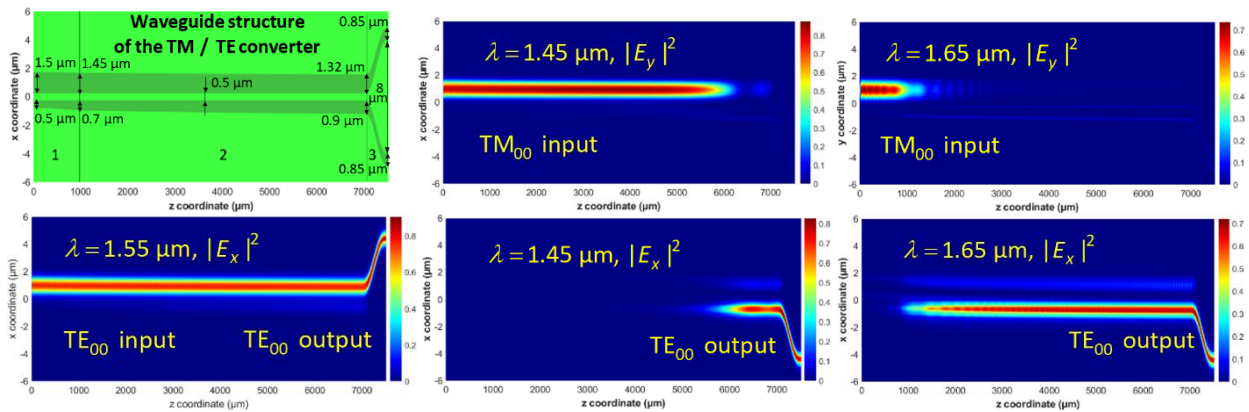


Fig. 3. Broadband adiabatic TM/TE splitter/converter. Waveguide structure and field distributions of the TM mode for the wavelengths  $1.45 \mu\text{m}$  and  $1.65 \mu\text{m}$  and of the TE mode for the wavelength  $1.55 \mu\text{m}$ .

The designed waveguide structure shown in Fig. 3 consists of a  $1000 \mu\text{m}$  linear taper section 1 ensuring sufficient decoupling of the input waveguides, the  $6000 \mu\text{m}$  long adiabatic mode evolution section 2, and the  $500 \mu\text{m}$  long output bends 3 separating the waveguides from the  $0.5 \mu\text{m}$  gap to edge-to-edge distance of  $8 \mu\text{m}$  and simultaneous tapering both waveguides to the output width of  $0.85 \mu\text{m}$ . In section 2, both waveguides are logarithmically tapered; the upper one from  $1.45 \mu\text{m}$  at the input to  $1.32 \mu\text{m}$  at the output while the bottom one from  $0.7 \mu\text{m}$  to  $0.9 \mu\text{m}$ . Fig. 3 also shows the conversion from the input  $TM_{00}$  mode of the upper waveguide to the input  $TE_{00}$  mode of the bottom one for wavelengths  $1.45 \mu\text{m}$  and  $1.65 \mu\text{m}$ . The  $TE_{00}$  input mode propagates essentially unaffected to the upper output branch for any wavelength in this band. The TM/TE coupler loss not exceeding  $0.2 \text{ dB}$  in the spectral range from  $1.45 \mu\text{m}$  to  $1.65 \mu\text{m}$  was calculated using the full-vector 3D Fourier modal method [9].

## BROADBAND 3-dB COUPLERS

To ensure the broadband operation, we implemented adiabatic mode evolution 3-dB couplers consisting of input adiabatic asymmetric waveguide bends followed by a mode evolution pair of waveguides linearly tapered to identical widths, which are then separated by symmetric bends. The design is shown in Fig. 4, together with the demonstration of its broadband operation. Numerical simulation using the Fourier modal method predicted the total loss lower than 0.05 dB and the splitting asymmetry lower than 0.2 dB in the whole spectral range.

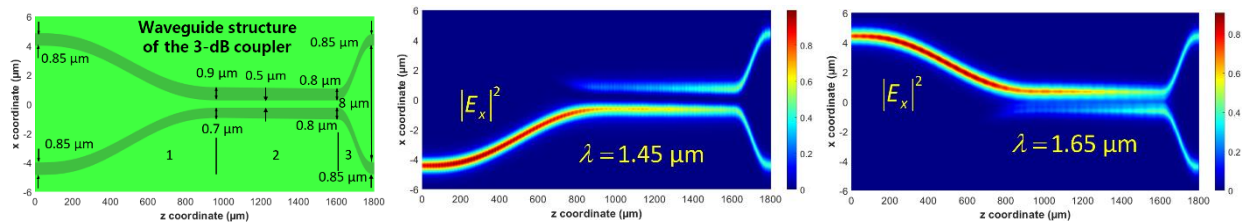


Fig.4. Broadband 3-dB coupler. Waveguide structure and field distributions at the wavelengths of 1.45  $\mu\text{m}$  and 1.65  $\mu\text{m}$ .

## ELECTRO-OPTIC PHASE SHIFTERS

Standard push-pull configuration of the electro-optic phase shifters is implemented. The designed electrodes are 6  $\mu\text{m}$  wide, separated by 1  $\mu\text{m}$  from the  $\text{Si}_3\text{N}_4$  stripe, and are composed of 150 nm  $\text{SiO}_2$  buffer covered with 200 nm of gold. Numerical simulations by COMSOL showed that the voltage of 1 V applied to the electrodes excites nearly uniform horizontal electric field intensity of  $2 \times 10^5$  V/m in the  $\text{LiNbO}_3$  slab. The distribution of the electric field is shown in Fig. 5. Optical absorption loss due to the presence of electrodes lower than 0.25 dB/cm and the half-wave voltage of the phase shifters lower than 5 V were predicted.

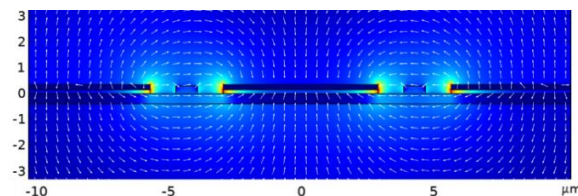


Fig. 5. Distribution of the DC electric field in the phase shifters.

## CONCLUSION

A successful proof-of-concept design of the broadband polarization controller based on the “etch-less”  $\text{Si}_3\text{N}_4$ -loaded thin film  $\text{LiNbO}_3$  was presented. An efficient polarization control was numerically demonstrated in the wavelength band from 1.45 to 1.65  $\mu\text{m}$  with low insertion loss and low operation voltage.

## References

- [1] R. Noé, H. Heidrich, and D. Hoffmann, *Automatic endless polarization control with integrated-optical Ti:LiNbO<sub>3</sub> polarization transformers*, *Opt. Lett.*, vol. 13, pp. 527-529, 1988.
- [2] A. Boes, B. Corcoran, L. Chang, J. Bowers, and A. Mitchell, *Status and Potential of Lithium Niobate on Insulator (LNOI) for Photonic Integrated Circuits*, *Laser & Photonics Reviews*, vol. 12, no. 4, p. 1700256, 2018.
- [3] Z. Lin *et al.*, *High-performance polarization management devices based on thin-film lithium niobate*, *Light Sci Appl*, vol. 11, no. 1, p. 93, 2022.
- [4] P. Zhang *et al.*, *High-speed electro-optic modulator based on silicon nitride loaded lithium niobate on an insulator platform*, *Opt. Lett.*, vol. 46, no. 23, pp. 5986-5989, 2021.
- [5] X. Han *et al.*, *Mode and Polarization-Division Multiplexing Based on Silicon Nitride Loaded Lithium Niobate on Insulator Platform*, *Laser & Photonics Reviews*, vol. 16, no. 1, 2021.
- [6] R. Gan *et al.*, *Fabrication tolerant and broadband polarization splitter-rotator based on adiabatic mode evolution on thin-film lithium niobate*, *Opt. Lett.*, vol. 47, no. 19, pp. 5200-5203, 2022.
- [7] H.-C. Chung, C.-H. Chen, Y. Hung, Jr., and S.-Y. Tseng, *Compact polarization-independent quasi-adiabatic 2×2 3 dB coupler on silicon*, *Opt. Express*, vol. 30, no. 2, 2022.
- [8] D. Guo and T. Chu, *Compact broadband silicon 3 dB coupler based on shortcuts to adiabaticity*, *Opt. Lett.*, vol. 43, no. 19, pp. 4795-4798, 2018.
- [9] J. Čtyroký, *3-D Bidirectional Propagation Algorithm Based on Fourier Series*, *J. Lightwave Technol.*, vol. 30, no. 23, pp. 3699-3708, 2012.